Supporting information for:

Understanding the Reactivity of Layered Transition Metal Sulfides: A Single Electronic Descriptor for Structure and Adsorption

Charlie Tsai,[†,‡] Karen Chan,[†,‡] Jens K. Nørskov,[†,‡] and Frank Abild-Pedersen[*,‡]

Department of Chemical Engineering, Stanford University, Stanford, California 94305, USA, and SUNCAT Center for Interface Science and Catalysis, SLAC National Accelerator Laboratory, Menlo Park, California 94025, USA

E-mail: abild@slac.stanford.edu

1 Calculation details

Structures were calculated using plane-wave density functional theory (DFT) employing ultrasoft-pseudopotentials as implemented in the QUANTUM ESPRESSO code.[S1] The BEEF-vdW exchange-correlation functional[S2–S5] was used for all calculations. A plane-wave cutoff and density cutoff of 500 eV and 5000 eV respectively were used. The bulk lattice constants are summarized in Table S1 and agree reasonably well with experimental values. The small discrepancy in the c parameter should not have a large effect on our results, since we consider only single layers. An infinite stripe model reported in previous studies[S6–S8] was used to investigate the M-edge and S-edge. When determining adsorption energies on one type of edge, the other edge had a constant structure.

Two unit cell sizes were used for the infinite stripe (Figure 1 of the main text): The larger unit cell consisted of four Mo atoms by four Mo atoms in the x and y direction respectively, while the smaller unit cell consisted of two Mo atoms by four Mo atoms in the x and y directions respectively. The larger unit cell was used to describe coverages of $\theta_H = 0.25$ and 0.75 ML and the smaller unit cell was used to describe coverages of $\theta_H = 0$, 0.5, and 1.0 ML. The adsorption of species other than H were all calculated on the larger unit cell. The MoS_2 stripes were separated by at least 9 Å of vacuum in the y-direction and 11 Å in the z-direction with periodic boundary conditions. The Brillouin zone was sampled by a Monkhorst-Pack $2 \times 1 \times 1$ and $4 \times 1 \times 1$ k-point grid for the large and small unit cells respectively.[S9] The structures were relaxed until all force components were less than 0.05 eV/Å. Spin-polarization was not considered.

---

[*]To whom correspondence should be addressed

[†]Department of Chemical Engineering, Stanford University, Stanford, California 94305, USA

[‡]SUNCAT Center for Interface Science and Catalysis, SLAC National Accelerator Laboratory, Menlo Park, California 94025, USA

Table S1: Theoretical and experimental lattice parameters for transition metal sulfides

Compound	Structure	Theoretical		Experimental		
		a	c	a	c	Reference
MoS_2	2H	3.19	13.05	3.162	12.29	S10
WS_2	2H	3.20	13.33	3.20	12.35	S11
NbS_2	2H	3.36	13.12	3.31	11.89	S10
TaS_2	2H	3.34	13.12	3.314	12.097	S12

With header "Lattice parameters (Å)" spanning the Theoretical and Experimental columns.

2 Adsorption energies

Differential adsorption energies are defined as:

$$\Delta E_H = E(\text{stripe} + \text{H}) - E(\text{stripe}) - \frac{1}{2}E(\text{H}_2) \tag{1}$$

$$\Delta E_S = E(\text{stripe} + \text{S}) + E(\text{H}_2) - E(\text{stripe}) - E(\text{H}_2\text{S}) \tag{2}$$

$$\Delta E_{SH} = E(\text{stripe} + \text{SH}) + \frac{1}{2}E(\text{H}_2) - E(\text{stripe}) - E(\text{H}_2\text{S}) \tag{3}$$

$$\Delta E_O = E(\text{stripe} + \text{O}) + E(\text{H}_2) - E(\text{stripe}) - E(\text{H}_2\text{O}) \tag{4}$$

$$\Delta E_{OH} = E(\text{stripe} + \text{OH}) + \frac{1}{2}E(\text{H}_2) - E(\text{stripe}) - E(\text{H}_2\text{O}) \tag{5}$$

$$\Delta E_{CHO} = E(\text{stripe} + \text{CHO}) - E(\text{stripe}) - E(\text{CO}) - \frac{1}{2}E(\text{H}_2) \tag{6}$$

$$\Delta E_{COOH} = E(\text{stripe} + \text{COOH}) - E(\text{stripe}) - E(\text{CO}_2) - \frac{1}{2}E(\text{H}_2) \tag{7}$$

$$\Delta E_{NNH} = E(\text{stripe} + \text{NNH}) - E(\text{stripe}) - E(\text{N}_2) - \frac{1}{2}E(\text{H}_2) \tag{8}$$

$$\Delta E_{NH_2} = E(\text{stripe} + \text{NH}_2) + \frac{1}{2}E(\text{H}_2) - E(\text{stripe}) - E(\text{NH}_3) \tag{9}$$

where "stripe" refers to the stable structures (summarized below) except for the S and N containing adsorbates, where "stripe" refers to the stable structure with one S atom removed to form a defect.

3 Stable edge structure determination

The stable S and H coverages of the edge are known to depend on the operating conditions. We follow a recently reported method of determining the edge structure under reducing conditions.[S13,S14] The free energy of each edge configuration γ was calculated using $\gamma = \left[G_{\text{stripe}} - \sum_i N_i \mu_i\right]/2L$, where the sum is over the number of atoms N and μ of all i constituents of the stripe in the unit cell of length L. We used the bulk TMS for all pure TMS structures. For doped MoS_2 we defined the free energy in terms of a reference edge, which was chosen to be $\theta_S = 0$ ML and $\theta_H = 0$ ML as the reference. Either way, γ is then

$$\gamma = \frac{1}{2L}\left(G_{\text{stripe}} - N_S\mu_S - N_H\mu_H\right) - \frac{G_{\text{stripe}}^{\text{ref}}}{2L} \tag{10}$$

where G_{stripe} is the free energy of the infinite stripe, and $G_{\text{stripe}}^{\text{ref}}$ is the reference. Under reducing conditions, the chemical potentials are determined by the following equilibrium reactions

$$2\left(\text{H}^+ + \text{e}^-\right) + \text{S}(^*) \rightleftharpoons \text{H}_2\text{S} + (^*) \tag{11}$$

and

$$\text{H}^+ + \text{e}^- \rightleftharpoons \text{H} \tag{12}$$

where $(^*)$ is a S vacancy. Following the computational hydrogen electrode approach (CHE),[S15,S16] the chemical potentials can be written in terms of the applied bias, U_{RHE} (defined relative to the reversible hydrogen electrode), as

$$\mu_{\text{H}} = \frac{1}{2}\mu_{\text{H}_2} - eU_{\text{RHE}} \tag{13}$$

and

$$\mu_{\text{S}} = \mu_{\text{H}_2\text{S}} - 2\mu_{\text{H}} = \mu_{\text{H}_2\text{S}} - 2\left(\frac{1}{2}\mu_{\text{H}_2} - eU_{\text{RHE}}\right) \tag{14}$$

where H_2S of 10^{-6} bar was chosen following standard corrosion resistance.[S17,S18]

The most thermodynamically stable edge configuration at $U_{\text{RHE}} = 0$ V was chosen (since we are interested in the low over-potential range in $U_{\text{RHE}} < 0$ V) according to their edge free energies γ, and then the stable coverage of H was taken to be where H_2 evolution is more exergonic than the desorption of $(^*)$SH as H_2S or further H adsorption. The evolution of H_2S should in reality be kinetically limited by hydrogen evolution at the S sites, since the pressure of H_2S is negligible under operating conditions, but MoS_2 catalysts have been found to be stable.[S8,S19,S20] We use a thermodynamic approximation to this kinetic process in this model since adsorption energies are known to scale with kinetic barriers.[S21,S22]

The coverages were defined as a fraction of a monolayer with respect to the available sites at the edge:

$$\theta_{\text{H}} = N_{\text{H}}/N_{\text{S}} \tag{15}$$

$$\theta_{\text{S}} = N_{\text{S}}/(2L) \tag{16}$$

where N is the number of atoms and L is the edge length. For structures with vacancies, the vacancy sites were counted as available sites instead of the S atom.

All structures are summarized below.

4   Summary of stable edge structures

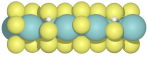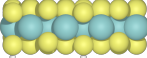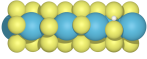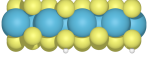Table S2: stable structures for various transition metal dichalcogenides
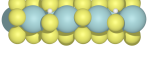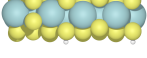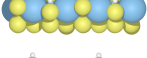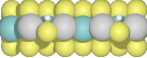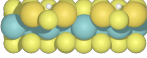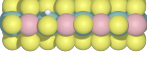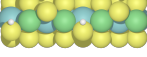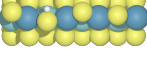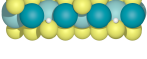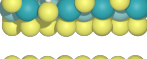
Edge	Structure	θ_S (ML)	θ_H (ML)	ε_d (eV)
MoS_2 Mo-edge		0.50	0.5	-0.73
MoS_2 S-edge		1.0	1.0	-0.89
WS_2 W-edge		0.50	0.25	-0.61
WS_2 S-edge		1.0	1.0	-0.48
NbS_2 Nb-edge		0.50	0.5	-0.09
NbS_2 S-edge		1.0	0.75	-0.20
TaS_2 Ta-edge		0.50	0.5	0.10
TaS_2 S-edge		1.0	1.0	0.01

Table S3: stable structures for doped MoS_2 S-edge

Dopant	Structure	θ_S (ML)	θ_H (ML)	ε_d (eV)
Ag		0.25	0.50	-3.92
Au		0.25	0.50	-3.18
Co		0.50	0.25	-1.10
Ni		0.50	1.0	-1.29
Os		0.50	0.25	-1.67
Pd		0.50	1.0	-2.33
Pt		0.50	1.0	-2.50
Rh		0.50	0.25	-1.85
Ru		0.50	0.50	-1.11

5 Relation between d-states and d_{yz} and $d_{x^2-y^2}$ states

We find that the d-band center scales with the weighted centers of the d_{yz} and $d_{x^2-y^2}$ states, which have been suggested to be especially important for the edge sites of MoS_2-type catalysts. The linear correlation between the states suggest that the d-band center is sufficient in describing the important features of these other states and either of them could work just as well as an electronic descriptor
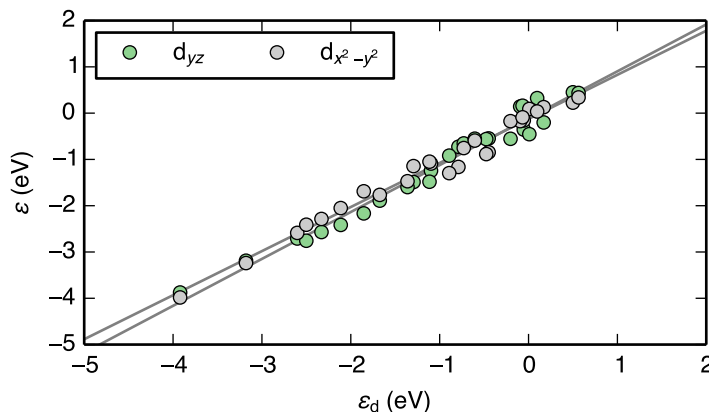

Figure S1: Plot of the d-band center ε_d vs. the d_{yz} center $\varepsilon_{d_{yz}}$ and the $d_{x^2-y^2}$ center $\varepsilon_{d_{x^2-y^2}}$. The quantities $\varepsilon_{d_{yz}}$ and $\varepsilon_{d_{x^2-y^2}}$ are defined in the same way as in ε_d except with the d_{yz} states and $d_{x^2-y^2}$ states, respectively.

References

(S1) Giannozzi, P.; Baroni, S.; Bonini, N.; Calandra, M.; Car, R.; Cavazzoni, C.; Ceresoli, D.; Chiarotti, G. L.; Cococcioni, M.; Dabo, I. et al. Quantum ESPRESSO: a modular and open-source software project for quantum simulations of materials. *J. Phys.: Condens. Matter* **2009**, *21*, 395502.

(S2) Wellendorff, J.; Lundgaard, K. T.; Møgelhøj, A.; Petzold, V.; Landis, D. D.; Nørskov, J. K.; Bligaard, T.; Jacobsen, K. W. Density functionals for surface science: Exchange-correlation model development with Bayesian error estimation. *Phys. Rev. B* **2012**, *85*, 235149.

(S3) Dion, M.; Rydberg, H.; Schröder, E.; Langreth, D. C.; Lundqvist, B. I. van der Waals density functional for general geometries. *Phys. Rev. Lett.* **2004**, *92*, 246401.

(S4) Thonhauser, T.; Cooper, V. R.; Li, S.; Puzder, A.; Hyldgaard, P.; Langreth, D. C. Van der Waals density functional: Self-consistent potential and the nature of the van der Waals bond. *Phys. Rev. B* **2007**, *76*, 125112.

(S5) Román-Péréz, G.; Soler, J. M. Efficient Implementation of a Van Der Waals Density Functional: Application to Double-Wall Carbon Nanotubes. *Phys. Rev. Lett.* **2009**, *103*, 096102.

(S6) Bollinger, M. V.; Lauritsen, J. V.; Jacobsen, K. W.; Nørskov, J. K.; Helveg, S.; Besenbacher, F. One-dimensional metallic edge states in MoS_2. *Phys. Rev. Lett.* **2001**, *87*, 196803.

(S7) Bollinger, M. V.; Jacobsen, K. W.; Nørskov, J. K. Atomic and electronic structure of MoS_2 nanoparticles. *Phys. Rev. B* **2003**, *67*, 085410.

(S8) Hinnemann, B.; Moses, P. G.; Bonde, J. L.; Jørgensen, K. P.; Nielsen, J. H.; Horch, S.; Chorkendorff, I.; Nørskov, J. K. Biomimetic Hydrogen Evolution: MoS_2 Nanoparticles as Catalyst for Hydrogen Evolution. *J. Am. Chem. Soc.* **2005**, *127*, 5308–5309.

(S9) Monkhorst, H. J.; Pack, J. D. Special points for Brillouin-zone integrations. *Phys. Rev. B* **1976**, *13*, 5188–5192.

(S10) Jellinek, F.; Brauer, G.; Müller, H. Molybdenum and Niobium Sulphides. *Nature* **1960**, *185*, 376–377.

(S11) Wildervanck, J. C.; Jellinek, F. Preparation and Crystallinity of Molybdenum and Tungsten Sulfides. *Z. Anorg. Allg. Chem.* **1964**, *328*, 309–318.

(S12) Meetsma, A.; Wiegers, G. A.; Haange, R. J.; de Boer, J. L. Structure of 2H-TaS$_2$. *Acta. Crystallogr. C Cryst. Struct. Commun.* **1990**, *46*, 1598–1599.

(S13) Tsai, C.; Chan, K.; Abild-Pedersen, F.; Nørskov, J. K. Active Edge Sites in MoSe$_2$ and WSe$_2$ Catalysts for the Hydrogen Evolution Reaction: A Density Functional Study. *Phys. Chem. Chem. Phys.* **2014**, *16*, 13156–13164.

(S14) Chan, K.; Tsai, C.; Hansen, H. A.; Nørskov, J. K. Molybdenum Sulfide and Selenides as Possible Electrocatalysts for CO$_2$Reduction. *ChemCatChem* **2014**, *6*, 1899–1905.

(S15) Nørskov, J. K.; Bligaard, T.; Logadóttir, Á.; Kitchin, J. R.; Chen, J. G.; Pandelov, S.; Stimming, U. Trends in the Exchange Current for Hydrogen Evolution. *J. Electrochem. Soc.* **2005**, *152*, J23–J26.

(S16) Peterson, A. A.; Abild-Pedersen, F.; Studt, F.; Rossmeisl, J.; Nørskov, J. K. How copper catalyzes the electroreduction of carbon dioxide into hydrocarbon fuels. *Energy Environ. Sci.* **2010**, *3*, 1311.

(S17) Pourbaix, M. *Atlas D'equilibres Electrochimiques*; Gauthier-Villars: Paris, 1963.

(S18) Hansen, H. A.; Rossmeisl, J.; Nørskov, J. K. Surface Pourbaix diagrams and oxygen reduction activity of Pt, Ag and Ni(111) surfaces studied by DFT. *Phys. Chem. Chem. Phys.* **2008**, *10*, 3722–3730.

(S19) Jaramillo, T. F.; Jørgensen, K. P.; Bonde, J. L.; Nielsen, J. H.; Horch, S.; Chorkendorff, I. Identification of Active Edge Sites for Electrochemical H$_2$ Evolution from MoS$_2$ Nanocatalysts. *Science* **2007**, *317*, 100–102.

(S20) Chen, Z.; Cummins, D.; Reinecke, B. N.; Clark, E.; Sunkara, M. K.; Jaramillo, T. F. Core–shell MoO$_3$–MoS$_2$ nanowires for hydrogen evolution: A functional design for electrocatalytic materials. *Nano Lett.* **2011**, *11*, 4168–4175.

(S21) Logadóttir, Á.; Rod, T. H.; Nørskov, J. K.; Hammer, B.; Dahl, S.; Jacobsen, C. The Brønsted–Evans–Polanyi Relation and the Volcano Plot for Ammonia Synthesis over Transition Metal Catalysts. *J. Catal.* **2001**, *197*, 229–231.

(S22) Bligaard, T.; Nørskov, J. K.; Dahl, S.; Matthiesen, J.; Christensen, C. H.; Sehested, J. The Brønsted–Evans–Polanyi relation and the volcano curve in heterogeneous catalysis. *J. Catal.* **2004**, *224*, 206–217.